Defect identification in GaAs grown at low temperatures by positron annihilation

J. Gebauer,[a] F. Börner, and R. Krause-Rehberg
Fachbereich Physik, Martin-Luther-Universität Halle-Wittenberg, D-06099 Halle, Germany

T. E. M. Staab
Laboratory of Physics, Helsinki University of Technology, P.O. Box 1100, FIN-02015 HUT, Finland

W. Bauer-Kugelmann, G. Kögel, and W. Triftshäuser
Institut für Nukleare Festkörperphysik, Universität der Bundeswehr München, D-85577 Neubiberg, Germany

P. Specht, R. C. Lutz, and E. R. Weber
University of California and Lawrence Berkeley Laboratory, Berkeley, California 94720

M. Luysberg
Institut für Festkörperforschung, Forschungszentrum Jülich, D-52425 Jülich, Germany

(Received 25 October 1999; accepted for publication 13 March 2000)

We use positron annihilation to study vacancy defects in GaAs grown at low temperatures (LT–GaAs). The vacancies in as-grown LT–GaAs can be identified to be Ga monovacancies, V_{Ga}, according to their positron lifetime and annihilation momentum distribution. The charge state of the vacancies is neutral. This is ascribed to the presence of positively charged As_{Ga}^{+} antisite defects in vicinity to the vacancies. Theoretical calculations of the annihilation parameters show that this assignment is consistent with the data. The density of V_{Ga} is related to the growth stoichiometry in LT–GaAs, i.e., it increases with the As/Ga beam equivalent pressure (BEP) and saturates at 2×10^{18} cm^{-3} for a BEP$\geqslant$20 and a low growth temperature of 200 °C. Annealing at 600 °C removes V_{Ga}. Instead, larger vacancy agglomerates with a size of approximately four vacancies are found. It will be shown that these vacancy clusters are associated with the As precipitates formed during annealing. © *2000 American Institute of Physics.* [S0021-8979(00)02812-7]

I. INTRODUCTION

GaAs layers grown by molecular beam epitaxy (MBE) at low temperatures (LT) (i.e., at 200–350 °C instead of 600 °C) exhibit unique properties like ultrashort carrier lifetimes[1] and high resistivity[2] after annealing. This can be attributed to the incorporation of up to 1% excess As during growth,[3] through the formation of native defects such as the As_{Ga} antisite, the Ga vacancy (V_{Ga}) and the As interstitial (As_i). The dominant defect species in LT–GaAs is the As_{Ga} antisite found in high concentrations of up to 10^{20} cm^{-3}.[4–6] Antisites can account for the nonstoichiometry as well as for the observed lattice expansion.[6] The well-known existence of positively charged As_{Ga}^{+} antisites implies the presence of compensating acceptors.[5,6] It was assumed that Ga vacancies, V_{Ga}, account for the compensation of As_{Ga}^{+}. V_{Ga} is expected to be a triple acceptor from theory[7] and should be favored in As-rich GaAs. If the Ga vacancies are indeed the dominant acceptors in LT–GaAs, the density of V_{Ga} must track that of the positively charged antisites. However, that was difficult to prove due to the lack of suitable experimental methods for the detection of vacancies.

Positron annihilation spectroscopy (PAS) using slow positrons is one of the few techniques to monitor type and concentration of vacancies in thin epitaxial layers.[8] Indeed, PAS showed the existence of vacancy defects in LT–GaAs (see, e.g., Refs. 9–11). However, the earlier studies lack a reliable identification of the vacancies detected, making quantitative interpretations difficult. In a previous work,[12] we related the vacancies in LT–GaAs to V_{Ga} by comparing the annihilation parameters to that of Ga vacancies in highly Si-doped GaAs. It was shown that the V_{Ga} density measured by PAS can quantitatively account for the compensation of As_{Ga}^{+}.[13] The defect concentrations of both, the As_{Ga} and the V_{Ga}, were found to increase with decreasing growth temperature, i.e., if the composition becomes more As rich. It was also shown that the concentration of As_{Ga} antisites is directly related to the As/Ga flux ratio or beam equivalent pressure (BEP) ratio during MBE growth. It is an open question whether the Ga vacancies exhibit a similar behavior. A direct relation between the V_{Ga} concentration and the elemental flux ratio would confirm the above picture, i.e., the compensation of As_{Ga}^{+} by Ga vacancies. Another interesting question is whether the Ga vacancy is part of a defect complex. This could not be decided from the previous positron experiments.

Annealing of LT–GaAs layers at temperatures of about 500–600 °C yields highly resistive layers.[2] This property has attracted much attention for device applications. During annealing, the density of the As_{Ga} antisites decreases[14,15] and the excess arsenic form precipitates.[16,17] It is still under debate whether the semi-insulating properties of annealed LT–

[a]Electronic mail: gebauer@physik.uni-halle.de

GaAs are due to the precipitates[17] acting as buried Shottky barriers or due to residual point defects which pin the Fermi level.[18] The role vacancies may play in annealed LT–GaAs is even more unclear. The formation of As precipitates has often been explained in terms of a V_{Ga} mediated diffusion of As_{Ga} antisites.[9,19] Positron annihilation results indicate the formation of defects larger than monovacancies during annealing.[10,11] It has been suggested that positron trapping in annealed LT–GaAs is related to As precipitates[20] whereas other authors interpreted their results in terms of isolated vacancy clusters.[10]

The use of LT–GaAs for different applications requires a proper understanding of the defects which determine the properties of the material. Our main goal is thus a reliable, detailed defect identification. In the present work we complete and extend our previous positron annihilation studies on vacancies in LT–GaAs. It turns out that we have to apply all available positron annihilation techniques. This includes standard Doppler-broadening measurements, also as a function of temperature, and positron lifetime spectroscopy using a pulsed positron beam. A major methodical improvement is the use of Doppler-broadening coincidence experiments which can be used to identify the chemical surrounding of the annihilation site. In addition to samples grown at different temperatures, we investigate samples grown with variable composition due to different As/Ga beam equivalent pressure (BEP) ratios. The defects in all as-grown samples investigated are found to be Ga monovacancies. They are most probably part of a neutral defect complex with As_{Ga} antisites. The density of the Ga vacancies increases with the BEP ratio and with decreasing growth temperature, i.e., if the composition becomes more As rich. Moreover, vacancies in annealed LT–GaAs are investigated. Of particular importance will be the use of Doppler-coincidence experiments. The dominant vacancy defects in annealed LT–GaAs are identified to be small vacancy clusters associated with the As precipitates. Ga monovacancies, however, appear not to be present in annealed LT–GaAs in significant concentrations.

II. EXPERIMENT

A. Sample material

The samples investigated in this study were grown by MBE in a Varian Gen-II system equipped with a diffusive reflectance spectroscopy DRS system for precise low growth temperature measurement. The growth rate was about 1 μm/h and the layer thickness was 1–2 μm. All samples were nominally undoped. The growth temperature (T_G) varied from 200 to 350 °C for samples grown with a BEP ratio of 20. An additional series with a BEP varying from 11 to 37 was grown at 200 °C. The BEP ratio can be determined with an accuracy of ± 2. A good crystalline quality was confirmed by high resolution x-ray diffraction measurements indicating pseudomorphic growth. Some samples of the growth temperature series were proximity annealed at 600 °C with the sample covered by another GaAs wafer to prevent As loss. A temperature of 600 °C was chosen because this is the usual temperature for epitaxial overgrowth in device applications.

In addition to the LT–GaAs layers, bulk reference samples were studied to obtain information about the annihilation characteristics of different defects. Highly Si-doped GaAs was used as a reference for Ga vacancies.[21] The existence of Ga vacancies in bulk GaAs is known to be related to the doping due to the Fermi-level effect. *n* doping enhances the equilibrium concentration of acceptor-type Ga vacancies. This is the reason for high concentrations of V_{Ga} in highly Si-doped GaAs.[22] On the contrary, *p*-type doping with, e.g., Zn decreases the concentration of acceptor-type Ga vacancies. In addition, it is expected that As vacancies are positively charged in *p*-GaAs and thus invisible for positrons.[7] Therefore, Zn-doped GaAs is expected to be free from positron trapping at vacancies. This is indeed commonly observed.[8,23] Therefore, GaAs:Zn is a suitable reference for the GaAs lattice. A semi-insulating GaAs sample containing vacancy clusters after plastic deformation is used as a reference for vacancy clusters in GaAs [12% deformation at 600 °C in (100) direction with a rate of 1.64×10^{-4} s^{-1}].[24] Metallic, polycrystalline As was observed as a reference for defects in the pure material. The samples were obtained from sintering 5 N As powder in a closed quartz ampoule at 600 °C.

B. Positron annihilation

During diffusion in a crystal positrons may be trapped by a vacancy. This results in an increase of the positron lifetime and a narrowing of the 511 keV annihilation peak compared to material free from trapping at vacancies. These effects can be used to determine concentration and type of vacancy defects.[8] Positron annihilation in thin LT–GaAs layers can only be observed by using slow, monoenergetic positrons with a well-defined penetration depth. Here, usually the Doppler broadening of the annihilation peak is observed as a function of incident positron energy. The annihilation peak was characterized by the lineshape parameters *S* and *W*. *S* is the fraction of annihilation with low momentum valence electrons having a longitudinal momentum $p_L < 3.2\times10^{-3}$ m_0c (m_0 is the electron rest mass and c the speed of light). *W* is the fraction of annihilation with high momentum electrons with 10.8×10^{-3} $m_0c < p_L < 15.5\times10^{-3}$ m_0c. Positron trapping in vacancies results in an increase (decrease) in *S* (*W*) since annihilation with low momentum valence electrons is increased at vacancies.[8] The absolute values of *S* and *W* depend on the definition of the momentum windows. Therefore, *S* and *W* are normalized to the values S_{bulk} and W_{bulk} found in a GaAs:Zn reference showing no positron trapping at vacancies. Even the normalized *S* and *W* depend slightly upon the special experimental arrangement (most important the resolution of the γ detector). One has to consider this fact when comparing Doppler-broadening data.[25]

Each defect type exhibits, in principle, its own specific *S* and *W* parameter, S_{defect} and W_{defect}. A measured *S* (or *W*) parameter is a superposition of contributions from different annihilation states. These contributions cannot be independently determined. Therefore, an identification of the vacancy which trapped the positron is not possible using the *S* parameter alone. If only one type of vacancy defects trap

positrons, the fraction η of positrons annihilating in vacancies can be written as

$$\eta=(S-S_{\text{bulk}})/(S_{\text{defect}}-S_{\text{bulk}})$$
$$=(W_{\text{bulk}}-W)/(W_{\text{bulk}}-W_{\text{defect}}). \quad (1)$$

Therefore, the measured S depends linearly on W if only the defect density changes (i.e., η), but not the defect type (i.e., S_{defect} and/or W_{defect}).[26] Such a linear $S-W$ variation is defect specific and can be used to identify a given vacancy defect by comparing the data with a reference. However, a certain probability remains to obtain different defect types with similar annihilation parameters or $S-W$ data lying on the same line. In order to exclude such uncertainties, positron lifetime measurements and Doppler-broadening coincidence spectroscopy were used in addition to the conventional $S-W$ analysis.

Provided only one type of defects traps positrons, the vacancy concentration can be obtained from the measured S parameter by

$$n_{\text{defect}}\mu_{\text{defect}}=\kappa=\lambda_b\frac{(S_{\text{defect}}-S)}{(S-S_{\text{bulk}})}, \quad (2)$$

where $\lambda_b=4.4\times10^9\ \text{s}^{-1}$ is the annihilation rate in defect-free GaAs.[8] The trapping coefficient μ_{defect} relates the positron trapping rate κ to the absolute vacancy concentration n_{defect}. The value $\mu_{\text{defect}}=1\times10^{15}\ \text{s}^{-1}$ is commonly accepted for negative monovacancies in semiconductors at room temperature.[27] Defect densities can also be estimated from the positron diffusion length L_+ via

$$n_{\text{defect}}\mu_{\text{defect}}=\kappa=\frac{D_+}{L_+^2}-\lambda_b, \quad (3)$$

where $D_+=1.8\ \text{cm}^2/\text{s}$ is the positron diffusion coefficient in GaAs. L_+ is ~200 nm in GaAs free from positron trapping at defects.[28]

The positron lifetime depends mainly on the electron density and provides direct information on the defect size.[8] Therefore, positron lifetime spectroscopy gives additional information on defects in comparison to Doppler broadening which is sensitive to the momentum distribution. A positron lifetime spectrum consists of a sum of exponential decay terms characterized by their respective intensities I_i and positron lifetimes τ_i. In defect free material a single lifetime τ_{bulk} is found ($\tau_{\text{bulk}}=1/\lambda_b=230$ ps in GaAs). If positrons are trapped in a vacancy, a second lifetime component, τ_{vac}, always longer than τ_{bulk}, is present. Therefore, an increase in the average positron lifetime $\tau_{\text{av}}=\Sigma I_i\tau_i$ above τ_{bulk} is a sign for positron trapping at vacancies.

Conventional Doppler-broadening spectra are dominated by background in the high momentum range at $p_L\geqslant15\times10^{-3}\ m_0c$. Doppler broadening coincidence spectroscopy, i.e., the coincident detection of both annihilation quanta, dramatically reduces the background in Doppler-broadening spectra.[29,30] This allows the observation of annihilation with high momentum core electrons up to $p_L\sim40-50\times10^{-3}\ m_0c$ which can be used to identify the chemical surrounding of the annihilation site.[30]

In addition to vacancies, positrons may be trapped in the attractive potential of negatively charged ions at low temperatures ($T\leqslant150$ K).[31] Also, positron trapping at negatively charged vacancies increases with decreasing temperature but is independent on temperature for neutral vacancies.[32] Therefore, PAS measurements as a function of temperature can be used to derive information on the charge state of vacancies as well as on the presence of negative ions.

C. Techniques

Doppler-broadening experiments were performed using a continuous slow positron beam. The incident positron energy was varied between 0.1 and 40 keV corresponding to a depth of ~0–2.5 μm. The temperature could be varied between 30 and 350 K using a closed-cycle helium cryocooler. About $6-8\times10^5$ events were usually collected in each spectrum. During the course of the present work two different γ detectors were used. The first one (used in our first study)[12] has a full width at half maximum (FWHM) of the resolution function of 1.45 keV (measured as the width of the ^{85}Sr-peak at 514 keV), better than the second with a FWHM of 1.6 keV, used for the samples grown with variable BEP ratio.

The positron lifetime as a function of depth (i.e., incident positron energy) was measured on some samples using a pulsed positron beam.[33] In this experiment, the incident positron energy was varied from 1 to 20 keV at room temperature. About 1×10^6 events were collected in each lifetime spectrum with a time resolution of 230 ps. Some bulk reference samples were investigated by conventional positron lifetime spectroscopy. A standard fast–fast spectrometer having a time resolution of about 230 ps was used. About $4-6\times10^6$ events were collected in each spectrum.

Doppler-broadening coincidence spectroscopy was performed on selected samples utilizing a setup of two Ge γ detectors with a system resolution of 1.1 keV and a peak to background ratio $\sim10^5$ (compared to 5×10^2 with one detector).[34] In this experiment the incident positron energy was fixed at 11 keV corresponding to a depth of ~0.35 μm to detect only annihilation from the LT–GaAs layer. 10^7 coincident events were recorded for each spectrum. The intensity of the annihilation with high-momentum core electrons was characterized by a W parameter calculated in the momentum range $(15-20)\times10^{-3}\ m_0c$.

Theoretical calculations of the annihilation characteristics were performed with the method introduced in Refs. 29 and 35. The high momentum distribution is calculated using the independent particle model within the generalized gradient approximation of positron annihilation.[36] Lattice relaxations were not taken into account. Theoretical W parameters are obtained from the calculated momentum distribution also in the range $(15-20)\times10^{-3}\ m_0c$. Positron lifetimes were calculated using the local density approximation.[37] A bulk lifetime of 225 ps for GaAs was obtained. The theoretical lifetimes are therefore scaled to the experimental bulk lifetime of 229 ps.[38]

The density of positively charged As_{Ga}^{+} antisites was determined via the magnetic circular dichroism of absorption (MCDA)[15] in the samples grown with variable As/Ga flux

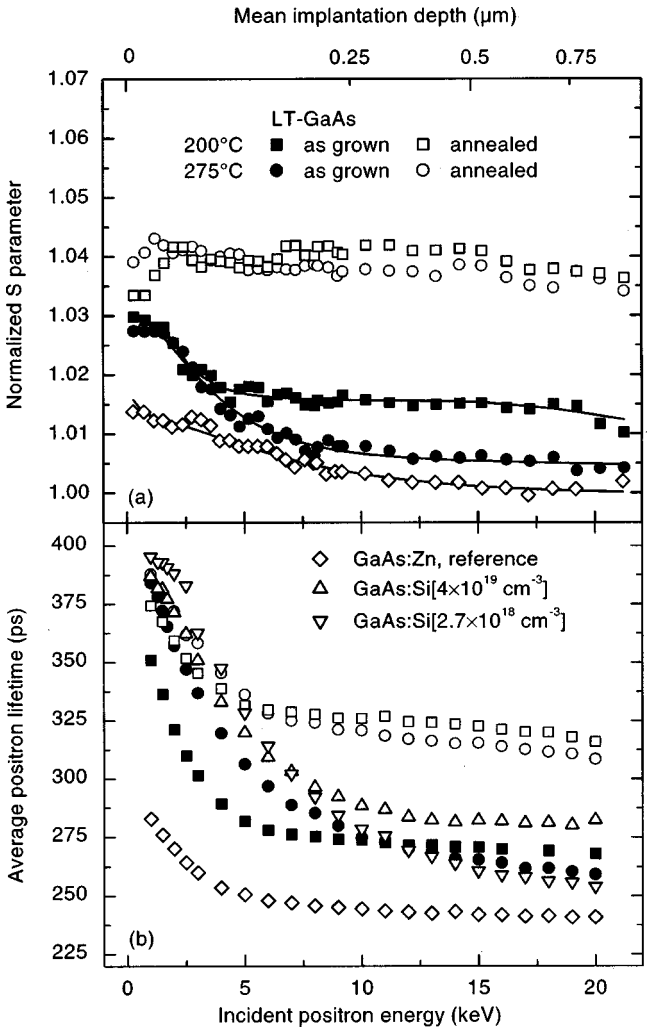

FIG. 1. (a) *S* parameter as a function of incident positron energy for LT–GaAs grown at 200 and 275 °C, as-grown and annealed in comparison to a Zn-doped GaAs reference free from positron trapping at vacancies. Solid lines are fits to the positron diffusion equation assuming a homogeneous defect density in the LT–GaAs layer. (b) Average positron lifetime as a function of incident positron energy for the same samples as in Fig. 1(a). In addition, the positron lifetime is shown for two GaAs samples highly doped with Si.

ratio. Structural investigation of As precipitates in annealed LT–GaAs were performed using a JEOL 4000FX electron microscope operating at 400 kV.

III. RESULTS

A. Detection of vacancies by Doppler broadening and positron lifetime spectroscopy

Figure 1(a) shows the normalized *S* parameter as a function of incident positron energy, *E*, as it is typically found in LT–GaAs.[12] The samples are grown at 200 and 275 °C and were also investigated after annealing at 600 °C. The change in $S(E)$ at low energies ($E<5-10$ keV) corresponds to the transition from positron annihilation at the surface to annihilation in the layer. The flat plateau of the *S* parameter observed at higher energies is characteristic for the LT–GaAs layer. The plateau values are well above the reference value measured in GaAs:Zn (open diamonds). This demonstrates clearly the presence of vacancy defects. No vacancies were detected in samples grown at temperatures higher than ~300 °C, neither as-grown nor annealed at 600 °C.

Solid lines in Fig. 1(a) are fits to the positron diffusion equation done with the VEPFIT program.[39] A homogeneous vacancy distribution in the layer according to the constant *S* is assumed. In the reference sample the positron diffusion length was $L_+=180(\pm 10)$ nm in agreement with the value $L_+=200$ nm obtained by others.[28] L_+ was shorter, i.e., 37 and 70 nm, in the 200 and 275 °C grown samples, respectively. Similar values of L_+ in LT–GaAs were reported by Fleischer *et al.*[40] The decrease of L_+ is directly visible in the $S(E)$ variation at low energies: the faster the transition from surface to bulk annihilation is, the shorter is L_+. A short diffusion length is indicative for a high density of positron traps [Eq. (3)]. *S* increases with decreasing growth temperature, T_G. This suggests an increasing density of vacancy defects with decreasing T_G in accordance to the decrease of L_+. *S* is low in the as-grown samples ($S\sim 1.005-1.02$) but increases after annealing ($S\sim 1.04$). This indicates defect reactions due to the thermal treatment.

Figure 1(b) shows the average positron lifetime, τ_{av}, measured in the same LT–GaAs samples in comparison to the standard Doppler-broadening measurements in Fig. 1(a). The positron lifetime in LT–GaAs behaves very similar to the *S* parameter. A decrease of τ_{av} is observed at low energies due to the transition from annihilation at the surface to annihilation in the layer. This allows a rough estimation of the positron diffusion length which follows similar trends as estimated from the *S* parameter measurements. In particular, L_+ is longer (~90 nm) in LT–GaAs grown at 270 °C than in LT–GaAs grown at 200 °C (~40 nm). The average positron lifetime in the LT–GaAs layers behaves like *S*: τ_{av} increases with decreasing T_G and the lifetime is much higher in annealed LT–GaAs (~325 ps) compared to as-grown material (~270 ps).

In addition to LT–GaAs the positron lifetime was also measured in highly Si-doped GaAs ([Si]$=2.7\times10^{18}$ and 4×10^{19} cm^{-3}). GaAs:Si serves as a reference for Ga vacancies because $V_{Ga}-Si_{Ga}$ complexes were identified in samples from the same wafers.[21] The annihilation parameters of the complexes are theoretically and experimentally known to be close to the ones of isolated V_{Ga}.[38,41] We must note that τ_{av} measured at high incident energies in GaAs:Zn and in GaAs:Si is 10–15 ps longer than observed by conventional positron lifetime spectroscopy in the bulk of the same samples. However, the results obtained with the lifetime beam exhibit the same relative changes of τ_{av}. Therefore, we attribute differences in the absolute lifetimes to differences between the two experimental setups. In addition, a long, surface-related positron lifetime (~400 ps) was detected in the positron beam lifetime experiments. The spectra for the GaAs:Zn reference were decomposed in two components and a bulk lifetime of 235 ps was found. This is in reasonable agreement with the value 230 ps found in conventional positron lifetime experiments.

In the higher Si-doped sample τ_{av} is known to be close to the saturation value for annihilation at V_{Ga} due to the high trapping rate (~1.4×10^{11} s^{-1}).[21] τ_{av} is slightly lower in the

LT–GaAs sample grown at 200 °C. The short diffusion length indicates a high trapping rate also in this sample ($\sim 0.8\times 10^{11}$ s^{-1}). That means, the vacancy-related lifetime (τ_{def}) in as-grown LT–GaAs is in the same range than in GaAs:Si. Because monovacancies were detected in GaAs:Si, the vacancies in LT–GaAs must also have an open volume like monovacancies. Positron trapping at defects larger than a monovacancy (having a larger τ_{def}) would result in a larger value of τ_{av} in LT–GaAs according to the high trapping rate. A decomposition of the lifetime spectra was performed with a fixed defect-related lifetime of 262 ps, typical for a monovacancy in GaAs[21] because an unconstrained decomposition of the lifetime spectra in LT–GaAs exhibited considerable statistical fluctuations.[42] The fit yielded a good variance, the intensity of the defect-related lifetime was in the order of 85% in accordance with the high trapping rate obtained from the L_+ analysis. The positron beam lifetime measurements show that the vacancies in as-grown LT–GaAs have an open volume like a monovacancy. Similar positron lifetime results in LT–GaAs were obtained in the positron beam lifetime study of Störmer *et al.*[43]

τ_{av} is about 325 ps in annealed LT–GaAs with small differences between material grown at 200 and 275 °C, very similar to the *S* parameter. A two-component analysis of the lifetime spectra yielded a defect-related lifetime of about 345 ps (intensity 85%) according to a trapping rate of ~ 2–3×10^{10} s^{-1}. The large value of the defect-related positron lifetime in annealed LT–GaAs indicates positron annihilation in an open volume larger than that of a monovacancy.

It is interesting to note that the surface *S* parameter and positron lifetime both converge to a similar point in most samples. However, the surface *S* parameter is somewhat lower than *S* in the annealed LT–GaAs layer, whereas the lifetime is distinctly higher at the surface than in the layer. A positron lifetime of 450–500 ps is generally associated with positron annihilation at surfaces.[8] However, the *S* parameter is more sensitive to the specific chemical environment. It is known that positron annihilation at oxygen-related defects leads to a reduction of *S* albeit with high positron lifetime.[44] Therefore, one might speculate that the differences are due to the thin oxide layer formed on GaAs when exposed to air.

B. Identification of Ga vacancies by a *S*–*W* analysis

In order to check more closely for the defect type and the number of different positron traps we performed a $S-W$ analysis as explained earlier [Eq. (2)]. The results are shown in Fig. 2 for a number of LT–GaAs samples grown at different temperatures and for some samples annealed at 600 °C. The respective *S* and *W* parameters were obtained from the plateau values between 10 and 15 keV incident positron energy [see Fig. 1(a)]. For as-grown LT–GaAs, all the $S-W$ data fall on the same straight line, indicating that only one defect-type traps positrons. The values agree with the values measured in highly Si-doped GaAs. This indicates the same defect type to be present in both types of materials. Because $V_{\mathrm{Ga}}-\mathrm{Si}_{\mathrm{Ga}}$ complexes were identified in GaAs:Si, we attribute the vacancies in LT–GaAs also to the Ga sublattice, i.e., to be Ga monovacancies.[12] The independent detection of monovacancies by the positron lifetime experiments supports this conclusion. The density of V_{Ga} was found to increase with decreasing growth temperature and reaches values of $\sim 2\times 10^{18}$ cm^{-3} at the lowest growth temperature (200 °C).[12]

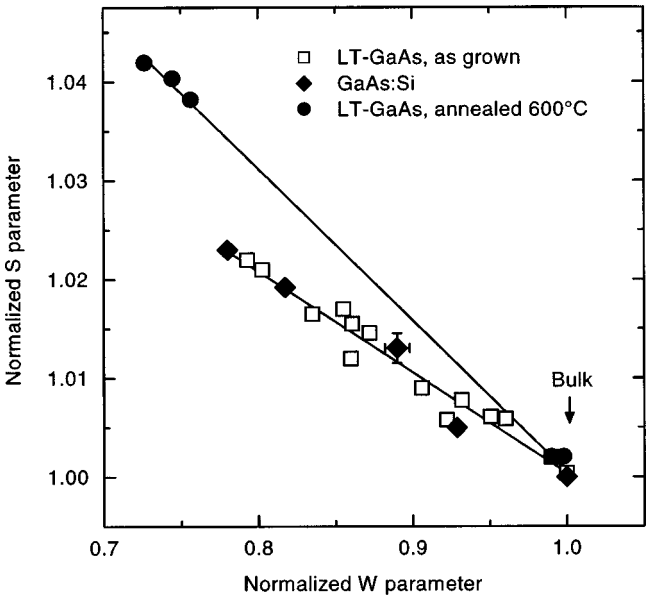

FIG. 2. *S* parameter vs the *W* parameter in LT–GaAs as-grown (□) and annealed at 600 °C (■) in comparison to highly Si-doped GaAs (◆) which serves as a reference for Ga vacancies. The linear variations, typical for the different defect type in the respective type of samples, are indicated. Each data point correspond to a different sample.

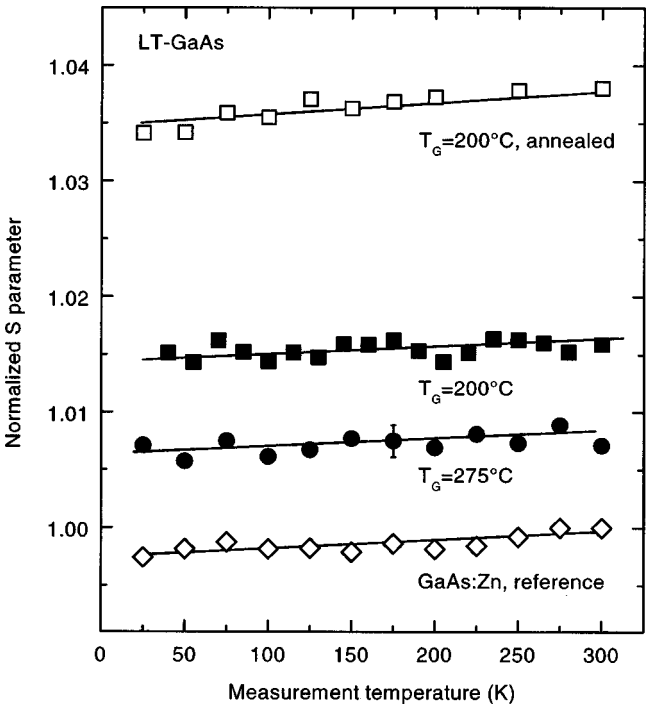

FIG. 3. *S* parameter as a function of the measurement temperature in as-grown and annealed LT–GaAs in comparison to a GaAs:Zn reference. The samples are indicated within the figure. Solid lines serve to guide the eye only.

The $S-W$ data in annealed LT–GaAs also show a linear dependence. However, the linear variation is clearly different from that in as-grown material. Thus, the defects are different from the Ga vacancies in as-grown material. This is consistent with the high positron lifetime and S parameter which indicates a larger open volume than that of monovacancies. Such defects are only detected in samples grown at $T \leqslant 300\,^{\circ}\mathrm{C}$. The samples grown above that temperature appear to be free of positron trapping after annealing, i.e., S and W are close to the bulk values. The linear variation in annealed LT–GaAs also contains the bulk values. This was confirmed by a $S-W$ analysis for each individual sample where all data points were found to be at the same line as shown in Fig. 2. Thus, in annealed LT–GaAs only one type of vacancy defects is present which dominates positron trapping. If a second defect type, i.e., Ga monovacancies, would be present, a deviation from the linear $S-W$ variation is expected. An upper limit of $\sim 10^{16}$ cm^{-3} for the V_{Ga} concentration in annealed LT–GaAs can be estimated. At this stage, it is not possible to estimate the concentration of the dominating vacancy defect in annealed LT–GaAs because the microscopic nature and thus the trapping coefficient are not known. In order to get more information about this defect we need the coincidence experiments shown in Sec. III E.

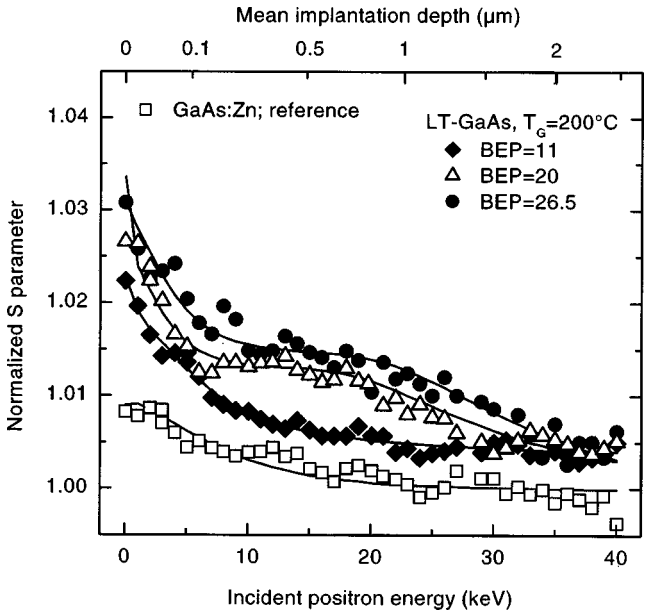

FIG. 4. S parameter as a function of the incident positron energy in LT–GaAs grown with variable stoichiometry (indicated by the BEP ratio) at 200 °C in comparison to a GaAs:Zn reference. Solid lines are fits to the positron diffusion equation assuming a homogeneous defect density in the LT–GaAs layer.

C. Revealing neutral Ga vacancy complexes by temperature-dependent measurements

Measurements as a function of temperature were performed on as-grown (200 and 275 °C) and annealed LT–GaAs. The results (S parameter in the LT–GaAs layer as a function of measurement temperature) are shown in Fig. 3 and compared to a GaAs:Zn reference. S increases slightly with increasing temperature in the reference. Here, positron annihilation takes place from the delocalized bulk state. The slight increase of the S parameter is therefore related to thermal lattice expansion.[8] The same weak temperature dependence is found in all LT–GaAs samples, only the absolute values of S are different. Thus, we attribute the slight increase of S with temperature in LT–GaAs to lattice expansion too, i.e., positron trapping at vacancies is independent of temperature in as-grown and annealed LT–GaAs. This is similar to the findings of Hautojärvi *et al.*[10] The results indicate also that positrons are not trapped by ion-type acceptors. The annihilation parameters for such defects are close to the bulk values but they can trap positrons only at low temperatures ($T<150$ K) in their shallow potential.[31] The presence of such defects would be detected as a strong decrease of S towards S_b with decreasing temperature. This is not found. Therefore, ion-type acceptors should not have a significant influence on the electrical properties of undoped LT–GaAs.

According to theory[7] and experiment,[23] Ga vacancies are negatively charged in GaAs when the Fermi level is close to midgap. One would therefore expect a strong temperature dependence of positron trapping in LT–GaAs. The lack of such temperature dependence indicates a neutral charge state of the vacancies.[32] There is also the possibility that the negative charge is screened by the large density of positively charged antisites. However, the $\mathrm{As}_{\mathrm{Ga}}^{+}$ concentration is in the order of some 10^{18} cm^{-3}. This is not enough to completely screen the Coulomb interaction.[27] Thus, screening by a homogeneous distribution of positively charged antisites can not explain our results. It follows that the vacancies are neutral. On the other hand, we demonstrated that the density of Ga vacancies correlates with the 1/3 of the $\mathrm{As}_{\mathrm{Ga}}^{+}$ concentration.[13] This shows that V_{Ga} indeed act as acceptor which compensates $\mathrm{As}_{\mathrm{Ga}}^{+}$. To resolve this puzzle, we have to conclude that the Ga vacancies in LT–GaAs are not isolated but surrounded with positively charged antisites, i.e., they behave like a neutral defect complex. This explains the lack of a temperature dependence of positron trapping as well as the compensation of $\mathrm{As}_{\mathrm{Ga}}^{+}$.

D. Vacancies in LT–GaAs grown with variable As/Ga flux ratio

In the following, investigations of LT–GaAs grown at 200 °C with variable As/Ga BEP ratio are presented. An increase of the BEP ratio is equivalent to a more As-rich composition. In Fig. 4(a), the S parameter is shown versus the positron energy for three representative samples of the BEP series. These measurements were performed with another γ detector than the earlier measurements. Due to the poorer resolution of the new detector, the quantities of the annihilation parameters are not directly comparable.[25] However, the results are qualitatively very similar to those obtained on samples grown at different temperatures: S exhibits a plateau characteristic for the LT–GaAs layer and is higher than in the reference sample. According to the earlier results, this is due to positron trapping at Ga vacancies. The decrease of S at higher incident energies is due to an increasing fraction of positrons annihilating in the substrate. Note that S does not reach the bulk value even at the highest incident positron

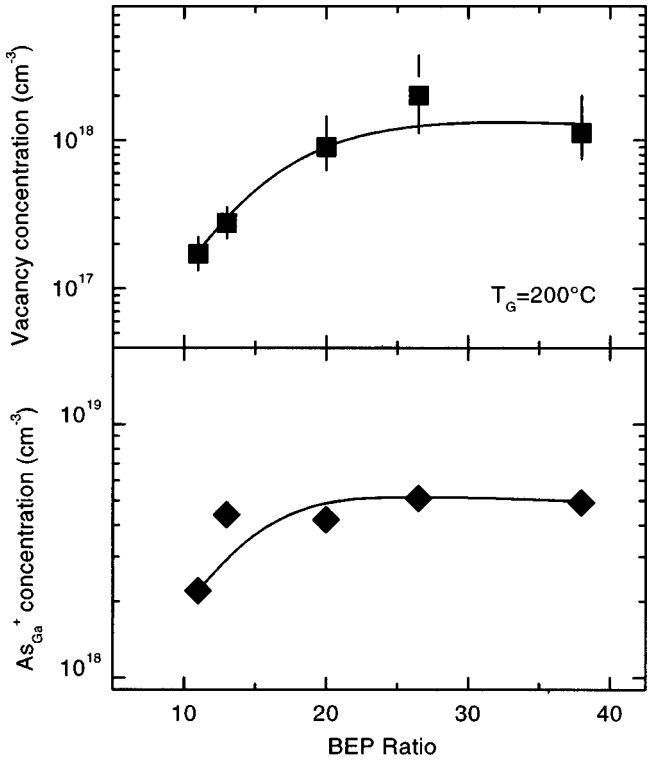

FIG. 5. (a) Concentration of Ga vacancies in LT–GaAs grown at 200 °C as a function of the BEP ratio during growth. (b) Density of positively charged As_{Ga}^{+} antisites determined by MCDA in samples from the same wafers. Solid lines are to guide the eye only.

energies, indicating the presence of vacancies in the substrate too. The reason is the use of highly Si-doped GaAs substrate ($[n]=10^{18}$ cm^{-3}). GaAs doped with Si by such amount is known to contain V_{Ga}–Si_{Ga} complexes at a level of $\sim 10^{17}$ cm^{-3}.[21] One could imagine that outdiffusion of Ga vacancies from the LT–GaAs layer increases the vacancy concentration in the substrate too. However, we found the same vacancy concentration in the substrate also for LT–GaAs samples containing no vacancy defects due to a high growth temperature ($T_g > 350$ °C). In that case, the S parameter in the layer was even below the value in the substrate. Therefore, defect diffusion appears to play only a minor role.

In Fig. 5(a) the vacancy concentration $[V_{Ga}]$ is shown as function of the BEP ratio for all samples grown with variable BEP. $[V_{Ga}]$ was determined from the S parameter in the LT–GaAs layer by using the trapping coefficient $\mu_{defect}=10^{15}$ s^{-1} in Eq. (3).[27] A S parameter of 1.017 for V_{Ga} was used for the calculation. This value is lower than that one of 1.024 determined earlier using the old γ detector.[12] The actual vacancy-related S parameter has been obtained from a renewed measurement on the highest Si-doped GaAs reference sample ($[Si]=4\times10^{19}$ cm^{-3}). Similar differences for $S(V_{Ga})$ have been found earlier for different experimental setups, see, e.g., Refs. 45 and 46.

The V_{Ga} concentration increases with the BEP ratio and reaches a value $[V_{Ga}]\sim 1-2\times10^{18}$ cm^{-3} at a BEP$\geqslant$20. $[V_{Ga}]$ is in good accordance to our earlier findings on samples grown at 200 °C with a BEP of 20.[12] The error bars in Fig. 5(a) are due to the statistical uncertainties of the S parameter only. They are thus a measure for the comparability of the PAS measurements. The true error for the vacancy concentration is larger due to systematic uncertainties which apply for all results. First, these are uncertainties of the vacancy-related and bulk S parameter S_v and S_b, respectively. Second, the trapping coefficient μ_{vac} is known with an accuracy of a factor of 2 only. This includes also the fact that the charge state of the vacancy should be neutral (see earlier). Therefore, a systematic error of at least a factor of 2 may apply for $[V_{Ga}]$. Note that the relative accuracy as indicated by the error bars is better.

In addition to the vacancy concentration, the density of positively charged As_{Ga} antisites $[As_{Ga}^{+}]$ was determined using MCDA[15] in samples from the same wafers. The results are shown in Fig. 5(b). For the determination of $[As_{Ga}^{+}]$ a systematic error of about 50% must be considered due to uncertainties imposed by the calibration.[13] $[As_{Ga}^{+}]$ increases with the BEP and saturates at $[As_{Ga}^{+}]\sim 5\times10^{18}$ cm^{-3} for a BEP$\geqslant$20. With the exception of the data point for BEP=13, $[As_{Ga}^{+}]$ is three times of the V_{Ga} concentration within the experimental errors. This is in agreement with the results in Ref. 13 where the same relationship between As_{Ga}^{+} and V_{Ga} concentration was found for samples grown at different temperatures. The results demonstrate a distinct relationship between As/Ga flux ratio and vacancy concentration in accordance with the variation of the As_{Ga}^{+} concentration.

E. Doppler-broadening coincidence measurements

1. Ga-vacancy complexes in as-grown LT–GaAs

In this section, we describe Doppler-broadening coincidence experiments to study the microscopic nature of the vacancies in as-grown LT–GaAs in more detail. In Fig. 6(a), the high momentum part of the annihilation momentum distribution is shown for the Ga vacancies in as-grown LT–GaAs in comparison to that of V_{Ga}–Si_{Ga} complexes in highly Si-doped GaAs. The data are normalized by taking the ratio to a GaAs:Zn reference because the momentum distribution itself spans several orders of magnitude, thus making a detailed comparison difficult.

The ratio curve for V_{Ga}–Si_{Ga} complexes increases at high momenta ($p_L > 12\times10^{-3}\ m_0c$), i.e., the momentum distribution decays less steeper than in the bulk (or, equivalent, it is narrower). This can easily be explained: in GaAs, the main contribution to the high momentum distribution comes from annihilation with As and Ga $3d$ electrons. In As ($Z=33$), the $3d$ electrons are stronger bound than in Ga ($Z=31$). Thus, the As $3d$ electrons have a broader momentum distribution with lower intensity. Because high momentum annihilation at Ga vacancies occurs mainly with $3d$ electrons from the neighboring As atoms, the momentum distribution should be broader than in the bulk. This is indeed observed in Fig. 4 for the Si_{Ga}–V_{Ga} complexes. The opposite behavior is expected for As vacancies, i.e., a momentum distribution narrower than in the bulk (corresponding to a decreasing ratio curve) due to the annihilation with $3d$ electrons from the surrounding Ga atoms.

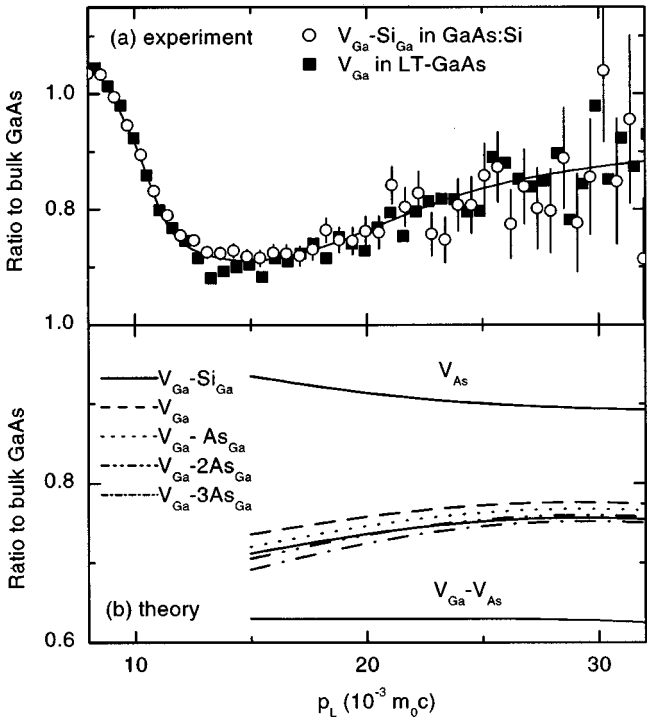

FIG. 6. (a) High-momentum part of the positron annihilation momentum distribution (normalized by taking the ratio to a GaAs:Zn reference) for Ga vacancies in a LT–GaAs sample ($T_G=200$ °C, BEP=20) and for $V_{Ga}-Si_{Ga}$ complexes in highly Si-doped GaAs. The measured spectra (total area 10^7 counts) were brought to unity area and scaled to full trapping at the vacancies. The fraction of trapped positrons was 0.95 in LT–GaAs and 0.9 in GaAs:Si. Solid lines are from data smoothing. (b) High-momentum part of the annihilation momentum distribution according to theoretical calculations for different vacancies and vacancy complexes in GaAs. The spectra are not accurate for $p_L < 15\times10^{-3}\ m_0c$ (see Ref. 35) and hence, are omitted.

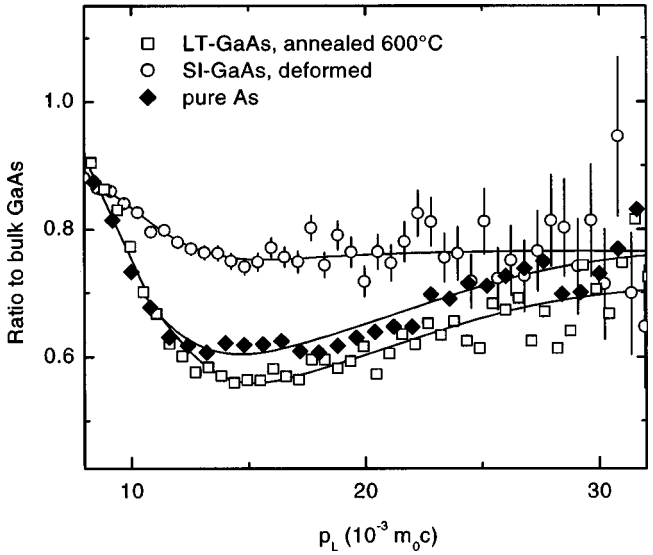

FIG. 7. High-momentum part of the positron annihilation momentum distribution for LT–GaAs ($T_G=200$ °C, BEP=20) annealed at 600 °C in comparison to metallic As and to semi-insulating GaAs containing vacancy clusters after plastic deformation (see Ref. 24). The spectra are as-measured, i.e., they are not scaled to full trapping. Solid lines are from data smoothing.

The momentum distribution for the vacancies in as-grown LT–GaAs agrees with that of the $V_{Ga}-Si_{Ga}$ complex within the experimental errors. This confirms independently the assignment to Ga vacancies. The W parameter is $W=0.73(1)$ for the $V_{Ga}-Si_{Ga}$ complexes and 0.72(2) for the Ga vacancy in LT–GaAs. Note that these values are different from those obtained in the conventional Doppler experiments due to the different experimental conditions and momentum windows.

The theoretical momentum distributions for Ga monovacancies and related complexes are shown in Fig. 6(b). The calculation of the momentum distribution is reliable only at $p_L > 15\times10^{-3}\ m_0c$ due to the use of atomic electron wave functions instead of the actual ones.[35] Corresponding W parameters and positron lifetimes are given in Table I. The shape of the theoretical momentum distribution for the $V_{Ga}-Si_{Ga}$ complex is in good agreement with the experiment and the theoretical W parameter ($W=0.72$) is similar to the experimental value ($W=0.73$). The calculation yields also very good agreement for the positron lifetime, i.e., 260 ps was calculated for $V_{Ga}-Si_{Ga}$ instead of the experimental value 262 ps.[21] This is a good test for the reliability of the theory because the $V_{Ga}-Si_{Ga}$ complexes were independently identified.[21]

The results of the temperature-dependent measurements suggest the existence of neutral complexes rather than of isolated Ga vacancies. Therefore, the momentum distribution was calculated for the isolated Ga vacancy and for defect complexes consisting of a Ga vacancy neighbored by 1–3 As_{Ga} antisites (denoted as $V_{Ga}-X$ As_{Ga} with $X=1-3$). W is slightly higher for V_{Ga} ($W=0.74$) compared to $V_{Ga}-Si_{Ga}$ (0.72), i.e., the momentum distribution has a higher intensity. However, the shape is practically the same. With increasing number of As_{Ga} antisites in a $V_{Ga}-X$ As_{Ga} complex, the intensity of the momentum distribution decreases slightly [Fig. 6(b)] but is close to that of V_{Ga}. The changes are in the same order than the experimental uncertainties in Fig. 1(a). Therefore, it is not possible to distinguish definitely between isolated Ga vacancies or $V_{Ga}-As_{Ga}$ complexes in as-grown LT–GaAs from the momentum distribution. However, the calculations show that the assignment to V_{Ga}- related defect complexes is compatible with the experimental data. Other vacancy defects can be ruled out according to shape and intensity of the momentum distribution, e.g., V_{As} or larger defects like $V_{Ga}-V_{As}$ divacancies [Fig. 1(b)].

2. Positron trapping at As-precipitates in annealed LT–GaAs

In this section we show the results of Doppler-broadening coincidence spectroscopy on the vacancy defects in annealed LT–GaAs, performed to get more information about their chemical surrounding. The positron lifetime and conventional Doppler-broadening measurements discussed earlier provide only the information that these positron traps have an open volume comparable to small vacancy clusters, i.e., they are not Ga monovacancies. It has been suggested that these defects are associated with As precipitates[20] but it has often been assumed that these are just isolated vacancy clusters.[10,11]

In Fig. 7, the annihilation momentum distribution mea-

sured in annealed LT–GaAs is compared with that of different reference samples. The momentum distribution in annealed LT–GaAs at $p_L > 15\times10^{-3}\ m_0c$ is broader than in the bulk, i.e., the ratio in Fig. 7 increases. Interestingly, the shape is very similar to that of V_{Ga} found in as-grown material [Fig. 6(a)]. However, the intensity of the core annihilation is reduced according to the increase of the open volume. The measured W parameter is 0.58(1).

The shape of the momentum distribution in annealed LT–GaAs indicates annihilation with electrons from As as it is the case for V_{Ga}. This finding highlights the importance of correlated measurements because an unambiguous defect identification in LT–GaAs can (therefore) not be obtained from the momentum distribution alone. For that purpose, we need also the $S-W$ analysis and the positron lifetime results as shown earlier. The fact that the momentum distribution shows annihilation exclusively with As atoms also in annealed LT–GaAs is a somewhat unexpected result. At a vacancy cluster, necessarily consisting of a similar number of both As and Ga vacancies, positron annihilation is not expected to occur preferentially with electrons from only one element. Thus, the shape of the annihilation momentum distribution for vacancy clusters should be very similar to that in the bulk but with reduced intensity due to the large open volume. This is supported by theoretical calculations. The shape of the momentum distributions for a $V_{Ga}-V_{As}$ divacancy [see Fig. 6(b)] and that of a cluster consisting of 2 V_{Ga} and 2 V_{As} are similar to that in the bulk, i.e., the ratio is constant. Such behavior is also experimentally found in a semi-insulating GaAs sample which contains vacancy clusters after plastic deformation.[24] The average positron lifetime was high (356 ps) and a defect related lifetime of 490 ps was found according to large vacancy agglomerates. The momentum distribution in deformed GaAs has the same shape than the bulk distribution as expected from the earlier arguments. However, it disagrees clearly with the momentum distribution in annealed LT–GaAs. This suggests a different nature of the positron traps, i.e., in annealed LT–GaAs positrons are not trapped by isolated vacancy clusters but rather by open volume associated with or even inside the As precipitates.

At this stage, it would be desirable to have theoretical calculations of the annihilation parameters for As precipitates in a GaAs matrix. However, this would require detailed knowledge of all atomic positions within such a precipitate, especially for the interface. At present, this is not known with the necessary accuracy. Therefore, the discussion is restricted to qualitative arguments.

To support the assignment of the vacancy defects in annealed LT–GaAs to As precipitates, we investigated metallic polycrystalline As as a reference. The measured W parameter is $W(\mathrm{As}) = 0.62(1)$. The shape of the momentum distribution in As is remarkably close to that in LT–GaAs, i.e., it is also similar to that in V_{Ga}. This is in agreement with the expectation that the shape of the momentum distribution depends only on the chemical environment.[29,35]

The As sample was also investigated by conventional positron lifetime spectroscopy at room temperature. We found an average positron lifetime of 330 ps, much higher than the theoretical bulk lifetime in rhombohedral As (189 ps, Table I). Spectra decomposition gave two lifetime components, i.e., $\tau_1 = 192$ ps (intensity 32%) and $\tau_2 = 395$ ps (intensity 68%). The first lifetime is in good agreement with the theoretical result for the bulk lifetime whereas the lifetime of 395 ps must be attributed to larger vacancy clusters. These results are similar to those obtained in other metals after sintering.[47] The first lifetime is attributed to annihilation inside grains, i.e., in material which is mostly free of defects whereas the long second lifetime is due to large open volume associated with grain boundaries. According to the theoretical calculations (Table I), the lifetime corresponds to an open volume of at least four vacancies in As. Thus, the momentum distribution measured in the As sample is rather that of a larger open-volume defect in As than that of the bulk. Shape and intensity of the momentum distribution as well as the average positron lifetime are very similar in annealed LT–GaAs and in the pure As sample. Therefore, the defects should be also similar. We conclude that in annealed LT–GaAs positrons detect open volume defects with a size of about four monovacancies, but this open volume is associated with As precipitates.

TABLE I. Theoretically calculated W parameter (relative to bulk GaAs) and positron lifetimes for monovacancies, monovacancy-related defect complexes, vacancy clusters in GaAs, and for defects in metallic rhombohedral As. The lifetimes are scaled by a factor of 1.018 in order to mimic the experimental bulk lifetime of GaAs.

Defect	τ (ps)	W_{rel}
GaAs bulk	229	1
V_{As}	260	0.92
V_{Ga}	262	0.74
V_{Ga}–Si_{Ga}	262	0.72
V_{Ga}–As_{Ga}	262	0.73
V_{Ga}–2 As_{Ga}	262	0.72
V_{Ga}–3 As_{Ga}	262	0.71
V_{As}–V_{Ga}	315	0.62
2 V_{As}–2 V_{Ga}	357	0.50
As (bulk)	189	0.81
As–V_1	243	0.59
As–V_2	279	0.47
As–V_3	312	0.41
As–V_4	335	0.38

The existence of As precipitates in our samples was confirmed by transmission electron microscopy (TEM). Figure 8 is a TEM bright-field image of the LT–GaAs layer annealed at 600 °C. A homogeneous distribution of precipitates is observed displaying Moire-fringe contrast. The precipitates were identified to consist of rhombohedral As by means of quantitative evaluation of the Moire fringes. The average particle size is 3.7 nm, determined from high-resolution electron micrographs. The density of the precipitates was determined from bright-field images obtained under two beam imaging conditions. The local sample thickness was determined from the extinction contours. The density of the precipitates was 10^{17} cm^{-3} with an error of about 20%.

It is known that the specific trapping rate scales linearly with the size of a vacancy cluster (i.e., it should be about four times larger for the As-precipitate-related vacancy clusters than for a monovacancy).[48] Thus, a positron trapping

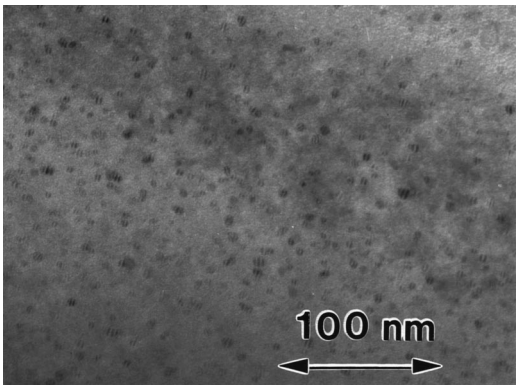

FIG. 8. TEM bright field image of As precipitates formed in a LT–GaAs layer ($T_G = 200\,^{\circ}\mathrm{C}$, BEP=20) after annealing at 600 °C.

rate in the order of $2\times10^{10}\ \mathrm{s}^{-1}$ is expected, in good agreement with the observation in annealed LT–GaAs (Sec. III A). Therefore, the assumption of positron trapping at As-precipitate-related vacancy clusters is also quantitatively compatible with the experiments.

IV. DISCUSSION

Our combined positron annihilation data, i.e., standard Doppler-broadening spectroscopy, positron lifetime, and Doppler-broadening coincidence spectroscopy reveals the existence of Ga monovacancies in as-grown LT–GaAs. This is in accordance to the assumptions in the earlier PAS studies.[9–11,40,49] Due to the combination of different techniques in conjunction with theoretical calculations in the present study, the identification of V_{Ga} can now be considered to be well established. Positron lifetime spectroscopy showed that the defects are monovacancies, whereas the conventional $S-W$ analysis shows that they belong to the Ga sublattice. This identification was independently confirmed by Doppler-broadening coincidence spectroscopy in conjunction with theoretical calculations.

Ga vacancies in electron irradiated GaAs are known to be mobile even below room temperature.[50] Therefore, a high concentration of vacancies such as in our samples would not be expected, unless defect complexes are formed which are known to be more stable.[51] Indeed, the measurements as a function of temperature indicate the formation of neutral defect complexes, probably with one or more $\mathrm{As_{Ga}}$ antisites. Theoretical calculations of annihilation parameters for V_{Ga}–$\mathrm{As_{Ga}}$ complexes are close to the experimental results. In a recent study, Korona[52] suggested a spatial correlation between $\mathrm{As_{Ga}^{+}}$ antisites and negative acceptors in LT–GaAs based on a numerical analysis of electron mobility data. Note that such defect correlation is sufficient to explain our results because the long range Coulomb interaction between positrons and vacancies would be effectively screened, even without the formation of closely bounded defect complexes. This result supports our interpretation. In a very recent study, Laine *et al.*[53] came to similar conclusions. It is interesting to note that the assignment of V_{Ga} in LT–GaAs to defect complexes has some analogies with the presence of donor-Ga-vacancy complexes in *n*-doped GaAs.[21,38] Such similarity was also suggested by Hurle in a recent review.[54]

Our previous studies show that the V_{Ga} concentration increases with decreasing growth temperature.[12] This can be understood as being related to the layer composition because LT–GaAs becomes more As-rich with decreasing T_G. In the present work, the V_{Ga} concentration is additionally found to be related to the elemental flux ratio. The V_{Ga} density in our samples saturates at a BEP$\geqslant$20. Similar, it was found that the $\mathrm{As_{Ga}}$ density increases with the BEP and saturates at BEP $\sim$20.[13] It is expected that, if V_{Ga} is the dominant acceptor in LT–GaAs, the density should track that of the $\mathrm{As_{Ga}}$ antisites. The present work and the results in Ref. 13 provide direct experimental evidence that this is indeed the case for a wide variety of growth conditions.

The temperature-dependent measurements show that ion-type acceptors are not detected in significant concentrations in LT–GaAs. It appears possible that such defects form neutral defect complexes too as discussed earlier for V_{Ga}. However, with the knowledge that the electrical compensation of $\mathrm{As_{Ga}^{+}}$ can be quantitatively explained by the Ga vacancies,[13] we can conclude that negative ions do not play a significant role for the electrical compensation in undoped LT–GaAs. Negative ions acting as shallow positron traps are normally attributed to impurities[21] or to intrinsic $\mathrm{Ga_{As}^{2-}}$ antisites.[31] The concentration of impurities is low in our MBE-grown layers whereas $\mathrm{Ga_{As}}$ antisites are not expected with the strongly As-rich stoichiometry of LT–GaAs. In a recent theoretical study, Landman *et al.*[55] found a low formation energy for a split As interstitial which could, therefore, be an abundant defect in the strongly As-rich LT–GaAs. Indeed, the excess As in LT–GaAs is sometimes related to interstitial-type defects[56] although a direct and unambiguous experimental evidence for their existence is still lacking. According to theory, the split interstitial should be an acceptor with a $0/-$ ionization level below that of the $\mathrm{As_{Ga}}$ antisite.[55] Thus the defect should be negatively charged in LT–GaAs where the Fermi level is pinned at the $\mathrm{As_{Ga}}$ level. Since we found no sign of ion-type acceptors, either the position of the ionization level is not correct or such interstitial defects does not exist in large concentrations in accordance to Ref. 6.

From a technological point of view, the detailed identification of vacancy defects in LT–GaAs opens up the possibility for future applications, e.g., to monitor growth and quality of similar layers by positron annihilation. This might be especially important for *in situ* characterization.[8]

After annealing at 600 °C, a positron trap different from Ga monovacancies is found. The high *S* parameter and positron lifetime indicate defects having a relatively large open volume. This increase of open volume during annealing was often simply interpreted in terms of vacancy clustering.[10,11] However, in order to form stable vacancy clusters, it would be necessary to supply As vacancies in addition to the already existing V_{Ga}. It is not obvious which mechanism could produce As vacancies in the strongly arsenic-rich LT–GaAs layer because this would result in the formation of additional defects, i.e., $\mathrm{As_{Ga}}$ antisites or As interstitials. Indeed, the results in Sec. III E 2 show clearly that positron trapping is not

due to isolated vacancy clusters but rather due to open volume associated with As precipitates. It is known that precipitation of excess As in LT–GaAs reduces the lattice strain present after growth.[6] Precipitation starts with the formation of coherent particles which, however, still induce a significant lattice dilation.[13,57] After annealing at ~600 °C, most precipitates undergo a structural transformation to rhombohedral As, thereby reducing lattice strain. Rhombohedral As is more closely packed than GaAs, i.e., the transition from coherent to rhombohedral precipitates must be accompanied by the buildup of open volume associated with the As precipitates. This provides an explanation for the open-volume defects detected by positron annihilation in annealed LT–GaAs because a large fraction of the As precipitates in our samples was found to be rhombohedral (Fig. 8). In addition, Ga vacancies existing in the as-grown material may be trapped at the precipitates during the annealing process. Such a trapping of vacancies might also reduce the lattice strain induced by coherent particles. In this sense, vacancies might also act as seeds for the precipitation process.

The open volume as seen by positrons in LT–GaAs annealed at 600 °C is probably too small to be seen by other structural sensitive techniques, e.g., electron microscopy. However, at higher annealing temperatures the open volume is expected to become larger. Indeed, vacancy clusters associated with As precipitates were found in LT–GaAs annealed at 800 °C[58] supporting the assignment given earlier.

V. SUMMARY

Positron annihilation was used to study native vacancy defects in GaAs grown at low temperatures. It was shown by the combined use of different positron annihilation techniques that the vacancies in as-grown LT–GaAs are Ga monovacancies. These vacancies are most probably part of a neutral defect complex, likely with As_{Ga} antisites. The density of the Ga vacancies increases if the layer composition becomes more As rich, i.e., with increasing BEP ratio. As it was the case for samples grown at variable temperatures, the concentration of V_{Ga} varies like the As_{Ga}-antisite concentration. No other acceptor-type defect was found by temperature-dependent measurements, whereas the concentration of V_{Ga} can explain the compensation of positive As_{Ga}^{+} antisites. After annealing at 600 °C, vacancy defects with an open volume larger than a monovacancy are found. It was shown that these defects are associated with the As precipitates formed during annealing. As the vacancy clusters dominate positron trapping, Ga monovacancies are not present in significant concentrations in annealed LT–GaAs. The results highlight the possibilities of positron annihilation to give detailed information about defect structures in thin layers and may thus serve as an example how such information may be extracted by the necessary combination of the different positron annihilation techniques and other spectroscopic and structural characterization tools.

ACKNOWLEDGMENTS

Financial support from the Bundesland Sachsen-Anhalt and from the Deutsche Forschungsgemeinschaft is acknowledged. The authors thank M. Hakala for providing the computer code for the theoretical calculation of the annihilation spectra and M. J. Puska for discussions regarding this point. T. E. M. S. thanks the European union for support in form of a Marie Curie grant. The research at UC Berkeley was supported by the Air Force Office of Scientific research, Grant No. F49620-98-1-0135. The use of the facilities of the Integrated Materials Laboratories at UC Berkeley is acknowledged.

[1] S. Gupta, M. Y. Frankel, J. A. Valdmanis, J. F. Whitaker, G. A. Mourou, F. W. Smith, and A. R. Calawa, Appl. Phys. Lett. **59**, 3276 (1991).
[2] F. W. Smith, A. R. Calawa, C. L. Chen, M. J. Manfra, and L. J. Mahoney, IEEE Electron Device Lett. **9**, 77 (1988).
[3] K. M. Yu, M. Kaminska, and Z. Liliental-Weber, J. Appl. Phys. **72**, 2850 (1992).
[4] M. Kaminska, Z. Liliental-Weber, E. R. Weber, T. George, J. B. Kortright, F. W. Smith, B. Y. Tsaur, and A. R. Calawa, Appl. Phys. Lett. **54**, 1881 (1989).
[5] H. J. von Bardeleben, M. O. Manasreh, D. C. Look, K. R. Evans, and C. E. Stutz, Phys. Rev. B **45**, 3372 (1992).
[6] X. Liu, A. Prasad, J. Nishio, E. R. Weber, Z. Liliental-Weber, and W. Walukiewicz, Appl. Phys. Lett. **67**, 279 (1995).
[7] S. B. Zhang and J. E. Northrup, Phys. Rev. Lett. **67**, 2339 (1991).
[8] R. Krause-Rehberg and H. S. Leipner, *Positron Annihilation in Semiconductors* (Springer, Berlin, 1999).
[9] D. E. Bliss, W. Walukiewicz, J. W. Ager, E. E. Haller, K. T. Chan, and S. Tanigawa, J. Appl. Phys. **71**, 1699 (1992).
[10] P. Hautojärvi, J. Mäkinen, S. Palko, K. Saarinen, C. Corbel, and L. Liszkay, Mater. Sci. Eng., B **22**, 16 (1993).
[11] D. J. Keeble, M. T. Umlor, P. Asoka-Kumar, K. G. Lynn, and P. W. Cooke, Appl. Phys. Lett. **63**, 87 (1993).
[12] J. Gebauer, R. Krause-Rehberg, S. Eichler, M. Luysberg, H. Sohn, and E. R. Weber, Appl. Phys. Lett. **71**, 638 (1997).
[13] M. Luysberg, H. Sohn, A. Prasad, P. Specht, Z. Liliental-Weber, E. R. Weber, J. Gebauer, and R. Krause-Rehberg, J. Appl. Phys. **83**, 561 (1998).
[14] D. C. Look, D. C. Walters, G. D. Robinson, J. R. Sizelove, M. G. Mier, and C. E. Stutz, J. Appl. Phys. **74**, 306 (1993).
[15] X. Liu, A. Prasad, W. M. Chen, A. Kurpiewski, A. Stoschek, W. Walukiewicz, E. R. Weber, and Z. Liliental-Weber, Appl. Phys. Lett. **65**, 3002 (1994).
[16] Z. Liliental-Weber, Mater. Res. Soc. Symp. Proc. **198**, 371 (1990).
[17] M. R. Melloch, N. Otsuka, J. M. Woodall, A. C. Warren, and J. L. Freeouf, Appl. Phys. Lett. **57**, 1531 (1990).
[18] D. C. Look, J. Appl. Phys. **70**, 3148 (1991).
[19] Z. Liliental-Weber, X. W. Lin, J. Washburn, and W. Schaff, Appl. Phys. Lett. **66**, 2086 (1995).
[20] N. Hozhabri, J. B. Bailey, A. R. Koymen, S. C. Sharma, and K. Alavi, J. Phys.: Condens. Matter **6**, L455 (1994).
[21] J. Gebauer, R. Krause-Rehberg, C. Domke, P. Ebert, and K. Urban, Phys. Rev. Lett. **78**, 3334 (1997).
[22] T. Y. Tan, H. M. You, and U. M. Gösele, Appl. Phys. A: Mater. Sci. Process. **56**, 249 (1993).
[23] C. Le Berre, C. Corbel, K. Saarinen, S. Kuisma, P. Hautojärvi, and R. Fornari, Phys. Rev. B **52**, 8112 (1995).
[24] C. G. Hübner, H. S. Leipner, O. Storbeck, and R. Krause-Rehberg, in *23rd International Conference on the Physics of Semiconductors*, edited by M. Scheffler and R. Zimmermann (World Scientific, Berlin, Germany, 1996), Vol. 4, p. 2805.
[25] S. Eichler and R. Krause-Rehberg, Appl. Surf. Sci. **149**, 227 (1999).
[26] L. Liszkay, C. Corbel, L. Baroux, P. Hautojärvi, M. Bayhan, A. W. Brinkmann, and S. Tatarenko, Appl. Phys. Lett. **64**, 1380 (1994).
[27] R. Krause-Rehberg and H. S. Leipner, Appl. Phys. A: Mater. Sci. Process. **64**, 457 (1997).
[28] E. Soininen, J. Mäkinen, D. Beyer, and P. Hautojärvi, Phys. Rev. B **46**, 13 104 (1992).
[29] M. Alatalo, H. Kauppinen, K. Saarinen, M. J. Puska, J. Mäkinen, P. Hautojärvi, and R. M. Nieminen, Phys. Rev. B **51**, 4176 (1995).
[30] P. Asoka-Kumar, M. Alatalo, V. J. Ghosh, A. C. Kruseman, B. Nielsen, and K. G. Lynn, Phys. Rev. Lett. **77**, 2097 (1996).
[31] K. Saarinen, P. Hautojärvi, A. Vehanen, R. Krause, and G. Dlubek, Phys. Rev. B **39**, 5287 (1989).

[32] M. J. Puska, C. Corbel, and R. M. Nieminen, Phys. Rev. B **41**, 9980 (1990).
[33] P. Willutzki, J. Stormer, G. Kogel, P. Sperr, D. T. Britton, R. Steindl, and W. Triftshauser, Meas. Sci. Technol. **5**, 548 (1994).
[34] J. Gebauer, R. Krause-Rehberg, S. Eichler, and F. Börner, Appl. Surf. Sci. **149**, 110 (1999).
[35] M. Alatalo *et al.*, Phys. Rev. B **54**, 2397 (1996).
[36] B. Barbiellini, M. Hakala, M. J. Puska, and R. M. Nieminen, Phys. Rev. B **56**, 7136 (1997).
[37] M. J. Puska and R. M. Nieminen, Rev. Mod. Phys. **66**, 841 (1994).
[38] J. Gebauer, M. Lausmann, T. E. M. Staab, R. Krause-Rehberg, M. Hakala, and M. J. Puska, Phys. Rev. B **60**, 1464 (1999).
[39] A. van Veen, H. Schut, J. Haakvoort, R. A. de Vries, and M. R. Ijpma, AIP Conf. Proc. **218**, 171 (1990).
[40] S. Fleischer, C. D. Beling, S. Fung, W. R. Nieveen, J. E. Squire, J. Q. Zheng, and M. Missous, J. Appl. Phys. **81**, 190 (1997).
[41] T. Laine, K. Saarinen, J. Mäkinen, P. Hautojärvi, C. Corbel, L. N. Pfeiffer, and P. H. Citrin, Phys. Rev. B **54**, 11 050 (1996).
[42] J. Gebauer *et al.*, Mater. Sci. Forum **255–257**, 204 (1997).
[43] J. Störmer, W. Triftshäuser, N. Hozhabri, and K. Alavi, Appl. Phys. Lett. **69**, 1867 (1996).
[44] M. Fujinami, Phys. Rev. B **53**, 13 047 (1996).
[45] K. Saarinen, S. Kuisma, P. Hautojärvi, C. Corbel, and C. LeBerre, Phys. Rev. B **49**, 8005 (1994).
[46] S. Kuisma, K. Saarinen, P. Hautojärvi, C. Corbel, and C. LeBerre, Phys. Rev. B **53**, 9814 (1996).
[47] T. E. M. Staab, R. Krause-Rehberg, B. Vetter, and B. Kieback, J. Phys.: Condens. Matter **11**, 1757 (1999).
[48] R. M. Nieminen and J. Laakkonen, Appl. Phys. **20**, 181 (1979).
[49] N. Hozhabri, S. C. Sharma, R. N. Pathak, and K. Alavi, J. Electron. Mater. **23**, 519 (1994).
[50] A. Polity, F. Rudolf, C. Nagel, S. Eichler, and R. Krause-Rehberg, Phys. Rev. B **55**, 10 467 (1997).
[51] R. Krause-Rehberg, H. S. Leipner, A. Kupsch, A. Polity, and T. Drost, Phys. Rev. B **49**, 2385 (1994).
[52] K. P. Korona, Acta Phys. Pol. A **88**, 643 (1995).
[53] T. Laine, K. Saarinen, P. Hautojärvi, C. Corbel, and M. Missous, J. Appl. Phys. **86**, 1888 (1999).
[54] D. T. J. Hurle, J. Appl. Phys. **58**, 6957 (1999).
[55] J. I. Landman, C. G. Morgan, J. T. Schick, P. Papoulias, and A. Kumar, Phys. Rev. B **55**, 15 581 (1997).
[56] R. E. Pritchard, S. A. McQuaid, L. Hart, R. C. Newman, J. Mäkinen, H. J. von Bardeleben, and M. Missous, J. Appl. Phys. **78**, 2411 (1995).
[57] Z. Liliental-Weber, A. Claverie, J. Washburn, F. Smith, and R. Calawa, Appl. Phys. A: Solids Surf. **53**, 141 (1991).
[58] S. Ruvimov, C. Dicker, B. J. Washburn, and Z. Liliental-Weber, Appl. Phys. Lett. **72**, 226 (1998).